Ferroelectric Phase Transitions in Ultra-thin Films of $BaTiO_3$

Jaita Paul[1], Takeshi Nishimatsu,[2,3,4] Y. Kawazoe[2] and Umesh V. Waghmare[1]
[1] *Theoretical Sciences Unit*
Jawaharlal Nehru Centre for Advanced Scientific Research
Jakkur PO Bangalore 560 064 India
[2] *Institute for Materials Research*
Tohoku University
Sendai, 980-8577, Japan and
[3] *Department of Physics and Astronomy, Rutgers University,*
136 Frelinghuysen Road, Piscataway, NJ 08544-8019
[4] *Japan Society for the Promotion of Science (JSPS) Post Doctoral Fellow for Research Abroad*

We present molecular dynamics simulations of a realistic model of an ultrathin film of $BaTiO_3$ sandwiched between short-circuited electrodes to determine and understand effects of film thickness, epitaxial strain and the nature of electrodes on its ferroelectric phase transitions as a function of temperature. We determine a full epitaxial strain-temperature phase diagram in the presence of perfect electrodes. Even with the vanishing depolarization field, we find that ferroelectric phase transitions to states with in-plane and out-of-plane components of polarization exhibit dependence on thickness; it arises from the interactions of local dipoles with their electrostatic images in the presence of electrodes. Secondly, in the presence of relatively bad metal electrodes which only partly compensate the surface charges and depolarization field, a qualitatively different phase with stripe-like domains is stabilized at low temperature.

PACS numbers:

Ferroelectric (FE) materials are vital to the technologies based on micro and nano electromechanical systems and certain random access memories. The fact that ferroelectricity in finite objects is very sensitive to mechanical and electrical boundary conditions is of great relevance to nano-scale devices based on ferroelectric materials [1, 2]. These boundary conditions in the case of a thin film are determined by the properties of its interfaces with substrate on which it is grown and the electrodes. While understanding the suppression of ferroelectricity in perovskite thin films has been a fundamental issue [3], a clever choice of an electrode and a substrate can be used effectively in designing nano-scale ferroelectric film based structures with desired properties. For example, a high-T_c lead-free ferroelectric was developed by growing $BaTiO_3$ films on an appropriate substrate [4].

FE materials are spontaneously polarized below a certain temperature and the direction of this spontaneous polarization can be switched by an external electric field [5]. When a FE film is polarized in a direction perpendicular to its plane, the bound charges at the surface of the film give rise to depolarization field that suppresses the spontaneous polarization. Free carriers in the interfacing electrodes partially compensate these surface charges, and aid in maintaining the ferroelectricity down to 6 unit cell thicknesses [6]. While the suppression of the out-of-plane polarization has been investigated fairly well [3, 4, 6] and can be understood with relative ease, effects of electrodes on the in-plane polarization and associated ferroelectricity have not been explored yet; their origin is expected to be fundamentally different. Since the switching of polarization necessary for memory applications occurs by rotation [7] through the states with in-plane polarization, understanding properties of these states is very important to applications of FE materials.

$BaTiO_3$, a standard example of FE perovskite [5], exhibits a sequence of phase transitions from cubic paraelectric to tetragonal (C<->T) to orthorhombic (T<->O) to rhombohedral (O<->R) ferroelectric phases characterized by polarization ordering along (001), (110) and (111) directions respectively. It is an ideal case for exploration of effects of electrodes, epitaxial strain and film thickness on in-plane ferroelectricity. Phenomenological Landau theory has been used to map a temperature-misfit strain phase diagram of $BaTiO_3$ and $PbTiO_3$ films of thickness > 50 nm grown on cubic substrate, with short circuit boundary conditions [8]. Diéguez et al., [9] mapped the equilibrium $BaTiO_3$ structure at zero temperature as a function of epitaxial strain and simulated corresponding ferroelectric transitions in the bulk using the effective-Hamiltonian approach [10, 11, 12]. Information about the strain-temperature phase diagram is very useful in the design of ferroelectric nano-structures.

In this letter, we use a first-principles model Hamiltonian of $BaTiO_3$ of Ref. 10 along with a simple electrostatic model of electrodes [13] in classical molecular dynamics simulations and determine (a) thickness dependence of ferroelectric transitions in $BaTiO_3$ films sandwiched between limiting cases of electrodes (perfect vs. imperfect), (b) a complete epitaxial strain-temperature phase diagram in the case of perfect electrodes and (c) the nature of low-temperature phase and ferroelectricity when the electrodes are not so perfect. We point out that interactions with electrostatic images of the in-plane dipoles interacting are responsible for size dependent ferroelectricity, even in the absence of depolarization field.

We used an effective lattice dynamical (phonon)

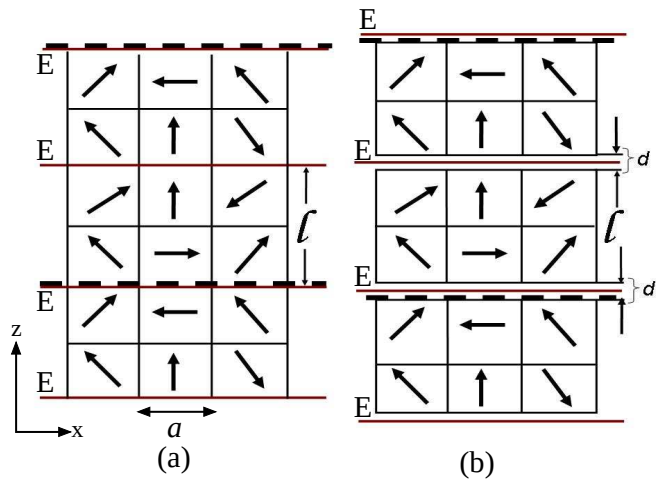

FIG. 1: Schematic representation of a FE thin film of thickness l unit cells (here l=2) sandwiched between (a) perfect and (b) imperfect electrodes. Horizontal thick lines marked as "E" represent the electrostatic mirrors used to model electrodes. They are distance $\frac{d}{2}$ away from the FE film surface (d=0 in (a), d=1 in (b)). Each arrow represents a local dipole within a unit cell (a=3.94 Å) of the FE crystal. Thick dashed lines indicate boundaries of the periodic box of the system used in simulations.

Hamiltonian of $BaTiO_3$ expressed in terms of localized atomic displacement basis spanned by two classical 3-dimensional vector degrees of freedom (DoF) per unit cell: one representing the unstable polar optical branches of the cubic structure and another representing the branches of acoustic phonons. This amounts to approximately integrating out the high energy phonons, reducing DoFs from 15 to 6 per unit cell. The average value of the former yields polarization, where as the latter describes local strains in the crystal. In addition, six components of the homogeneous strain tensor are included in the DoFs. This Hamiltonian includes harmonic and anharmonic interactions of phonons, coupling between polar and strain DoFs, and elastic contribution to energy. We use the parameters in effective Hamiltonian as determined earlier from first-principles local density functional theory calculations [10, 11]. Due to underestimation of lattice constant in this scheme, a negative pressure of -5 GPa is used in all simulations for comparison with experiment. An effective mass is attached to each polar DoF, based on the eigenvector of the unstable mode at $\Gamma-$point and ionic masses.

To model a FE thin film sandwiched between two electrodes, we have treated electrodes as perfect electrostatic mirrors located at a distance $\frac{d}{2}$ away from the surface of the film (see Fig. 1). This "gap" can also be thought of as a dead layer separating electrodes from the FE film. The length-scale d determines how effective the electrodes are in compensating the depolarization field [13]:

$$E_d = -4\pi \frac{d}{l+d} P_z \hat{z} \qquad (1)$$

where P_z is the out-of-plane polarization in the film, l being the thickness of film (both l and d are in the units of number of unit cells). Here, we use two limiting values of d: $d = 0$ corresponding to "perfect" electrodes and vanishing depolarization field, and $d = 1$ corresponding to "bad" electrodes on the $BaTiO_3$ thin films. It is clear that an electrostatic image of an electric dipole in the FE film is a dipole with same magnitude inside the electrode. However, the direction of the image dipole is the same (opposite) as that of the dipole in the film, if it is in z (x or y) direction. In this work, we consider identical electrodes on the two sides of the FE film, which allows simulations with periodic boundary conditions (due to infinite number of images, see Fig.1) with a periodicity of $2(l+d)$, i.e., treatment of electrodes amounts to simulating periodic system with twice the size of the film. We simulated FE films of two types: (a) bulk-like (system F) which have no epitaxial constraint and can be strained in the plane of the films, and (b) epitaxial films (system EF), whose in-plane strain is fixed by the choice of the substrate (electrode). We keep the in-plane homogeneous strain DoF fixed during the simulation of the latter. As a check on internal consistency and for comparison, we also simulated ferroelectricity in bulk $BaTiO_3$ (system B) with the same size(s) using periodic (*not mirror*) boundary conditions (note that there are no electrodes in system B, unlike in systems F and EF).

Mixed-space molecular dynamics, used earlier in large-scale simulations of relaxors [14, 15] treating infinite-range dipolar interactions in reciprocal space, is used here to determine finite temperature properties of the effective Hamiltonian. The Nosè-Poincarè [16] thermostat with simplectic properties implemented in the present simulations allows us to use a relatively large timestep of 2 femtoseconds. At each temperature, the system was thermalized with 50,000 timesteps and averaging was performed using configurations of subsequent 150,000 timesteps (amounting to a simulation of 0.3 nano sec). Since ferroelectric phase transitions are known to be first-order and exhibit hysteresis, we increased (decreased) temperature in small steps of 10 to 20 K in the heating (cooling) runs of simulations, with smaller temperature steps near the transition. The size of systems in our simulations is $16 \times 16 \times l$, where $l = 2, 11$ unit cells.

We first report our results for FE films sandwiched between perfect electrodes: $d = 0$. In the limit of large thickness, ferroelectric properties of thin films with no epitaxial constraint (system F) are expected to converge to the bulk behavior. We find for both the systems F and B that the transition temperatures do depend on the thickness for polarization ordering in all the three directions of polarization (Fig. 2a). The dependence of T_c of the system B arises from the statistical mechanical effects of the finite size [17], where as the difference between the T_c's of systems B and F reveal the nano-size effects of the film thickness. It is evident that the transitions to FE states with in-plane polarization occurring at higher temperatures in the films converge to bulk

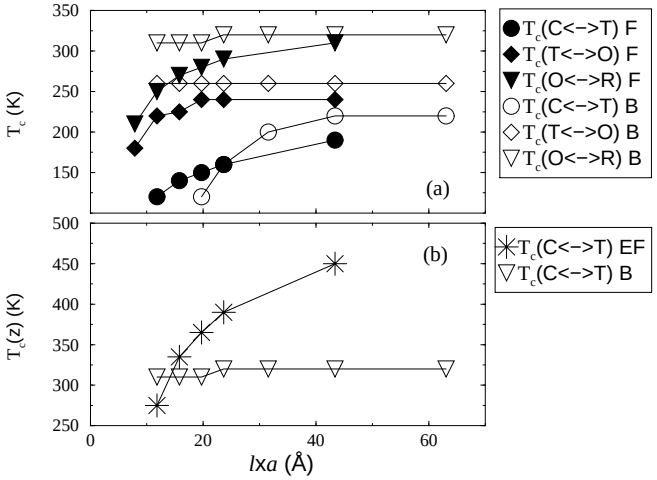

FIG. 2: Dependence of transition temperatures on the thickness of films sandwiched by perfect electrodes (a) with no and (b) with epitaxial constraint (B: Bulk, given for comparison, F: Film without epitaxial strain, EF: Films with epitaxial strain): a = lattice constant of $BaTiO_3$.

behavior when the film thickness is greater than 10 unit cell layers, where as the transition to the state with out-of-plane polarization converges more gradually to that in the bulk. This dependence of $T_c(z)$ on the film thickness even in the case of vanishing depolarization field is surprising.

A related finding from our simulations is that even the high temperature paraelectric phase $P = 0$ of films F exhibits tetragonality through uniaxial symmetry of its dielectric constant. The origin of both the findings can be traced to the fact that electrostatic images of the in-plane local dipoles in the presence of electrodes are inverted and break the horizontal reflection symmetry σ_h. Since these images interact with local dipoles in the film polarized in any general direction, in a way distinct from that in the bulk, the presence of electrodes gives rise to thickness dependence of ferroelectric transitions in films even in the absence of depolarization field.

We find a rather different thickness dependence of the ferroelectric transition behavior in epitaxial $BaTiO_3$ films sandwiched between perfect electrodes (see Fig. 2b). In this case, the in-plane strain is clamped which suppresses the fluctuations associated with in-plane dipole moments (FE transitions are fluctuation driven first-order phase transitions [12]) and hence the transition temperature for in-plane ordering is reduced, which remains almost constant at 70 K ($\pm$10 K) as a function of film thicknesses. Unlike bulk, there is no orthorhombic phase stable at intermediate temperatures. Epitaxial constraint naturally favors uniaxiality, resulting in a noticeable enhancement of the temperature of the transition (well above the bulk transition) to the state with out-of-plane polarization, consistent with experimental observations [4]. Our simulations suggest a critical thickness of 3 unit cell layers, below which we find no ordering of P_z at low temperatures.

The value of epitaxial strain has a spectacular effect on ferroelectric phase transitions in the films (see Fig. 3 for results in the presence of perfect electrodes $d = 0$). At compressive epitaxial strains ($\epsilon_{xx} < -0.005$), $BaTiO_3$ films exhibit a single transition to tetragonal phase, with increasing T_c with the magnitude of strain. For $-0.005 < \epsilon_{xx} < 0.03$, they exhibit two transitions from paraelectric to tetragonal FE and then distorted rhombohedral FE phases ($R^{'}$) as the temperature is lowered. There is a crossover point at $\epsilon_{xx} = 0.012$, below (above) which the low temperature phase has $P_z > P_x = P_y$ ($P_z < P_x = P_y$); at this point, there is only one second order transition from cubic to rhombohedral FE phase, which does not seem to depend on the film thickness. For $\epsilon_{xx} > 0.03$, there is a single phase transition to orthorhombic FE phase whose T_c increases with the magnitude of strain. Through comparison with the work of Diéguez et al [9], we show (a) the presence of perfect electrodes results in a shift in the temperature-strain phase diagram to the right along strain axis by roughly $\Delta\epsilon_{xx} \sim 0.012$, and (b) and there is an overall reduction in the transition temperatures by about 70 K partly due to the dependence on film thickness. General features of our phase diagram are closer to that determined by Diéguez et al [9] than the one of Pertsev et al [8]. We note that the low-temperature aspects of this phase diagram are consistent with properties of $BaTiO_3/SrTiO_3$ superlattice as a function of epitaxial strain [18].

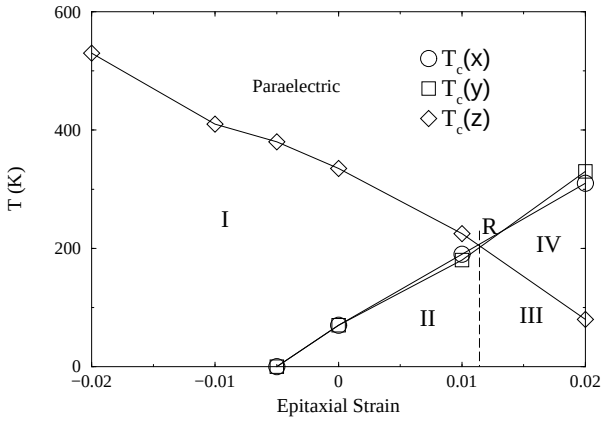

FIG. 3: Temperature-epitaxial strain phase diagram of a film (of 4 unit cell thickness) sandwiched between perfect electrodes ($d = 0$). Region I is tetragonal, II and III are the $R^{'}$ phase (see text and [Ref.8]), and IV is orthorhombic. Regions II (P_x (= P_y) < P_z) and III (P_x (= P_y) > P_z) are separated by a rhombohedral phase R.

Ferroelectricity in the ultra-thin films of $BaTiO_3$ sandwiched between "bad" electrodes ($d = 1$) is qualitatively different from its bulk behavior. In this case, the depolarization field is quite sizeable and effective in suppressing P_z. The dielectric constant (see Fig. 4, top panel) ϵ_{zz} exhibits a divergence near $T = 0$ K, but no signature of a phase transition to a ferroelectric state with polarization

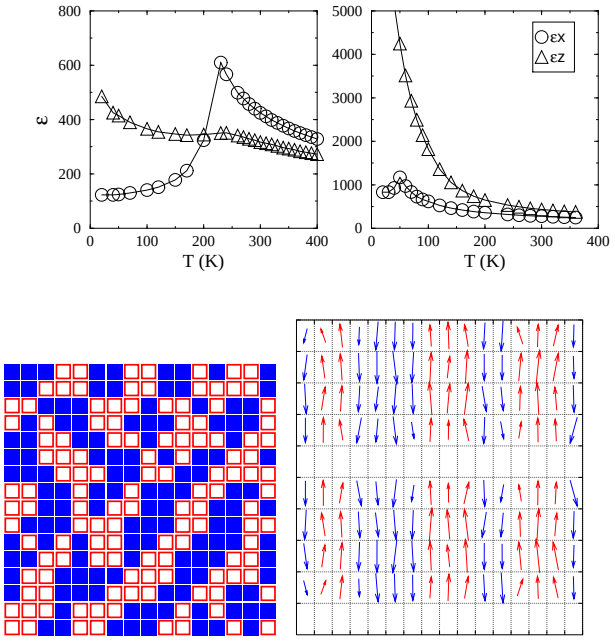

FIG. 4: Top: Dielectric constant as a function of temperature for (left) films (F) and (right) epitaxial films EF (l=4, d=1), sandwiched between "bad" electrodes. Bottom: A horizontal slice on the left ($+z$ and $-z$ polarized sites are symbolized by empty and filled boxes respectively) and a vertical cross-section on the right for $16 \times 16 \times 4$ system for the same configuration at 110 K showing domain formation.

P_z. The tetragonality of the high temperature paraelectric phase is also apparent in the uniaxial symmetry of dielectric constant. The transition to FE phase ordered with in-plane polarization occurs at around 70±10 K for epitaxial thin films. For the films without epitaxial constraint, this transition occurs at a higher temperature ($\sim$ 210 K). To understand the nature of low temperature phase with very high zz dielectric response, we examine the snapshots of dipolar configurations of these films. They reveal (Fig. 4, bottom panel) formation of vertical ((010) planes) stripe-like domains with polarization along $z-$axis which form arbitrary patterns in the (001) planes. Our results are very similar to those observed experimentally by Fong et al [3]. We find that these domains are stable throughout the duration of our simulation (about 0.1 nano sec) and observed at temperatures as high as 300 K. It is clear that these stripe-like domains are stabilized through minimization of the energy cost associated with depolarization field. Formation of similar domain structure was also predicted by Levanyuk et al [19].

Origin of most of our observations can be understood through Fourier analysis of the dipolar configurations noting the mirror boundary conditions and vanishing of dipoles in the gap region. For example, P_z can be only an even function, where as P_x is always an odd function of z; hence $q = 0$ component of P_x has to be zero (for the doubly periodic cell). This leads to fluctuations of the in-plane electric dipoles whose length-scale is determined by the film thickness. Since these dipoles couple with both the strain and out-of-plane dipoles, ferroelectricity even in the absence of depolarization field exhibits thickness dependence.

In summary, we have shown that the ferroelectricity in thin films sandwiched between electrodes exhibits nano-thickness dependence even if the depolarization field vanishes. Secondly, the presence of electrodes and their nature have wide-ranging consequences to ferroelectricity in ultra-thin films from simple size dependence to stabilization of phases with stripe-like domains. The origin of these phenomena lies in interaction between local dipoles and their electrostatic images in electrodes.

UVW thanks P. Ayyub and R. Budhani for useful discussion; TN thanks JNCASR for local hospitality. We thank International Frontier Center for Advanced Materials (IFCAM) of IMR who supported UVW to visit to Sendai and authors' collaborative study in ferroelectrics and the Centre for Computational Materials Science at JNCASR for financial support.

[1] J. F. Scott, C. A. P. de Araujo, Science **246**, 1400 (1989)
[2] C. H. Ahn, K. M. Rabe, J. M. Triscone, Science **303**, 488 (2004)
[3] D. D. Fong, G. B. Stephenson, S. K. Streiffer, J. A. Eastman, O. Auciello, P. H. Fuoss, C. Thompson, Science, **304**, 1650 (2004)
[4] K. J. Choi, M. Biegalski, Y. L. Li, A. Sharan, J. Schubert, R. Uecker, P. Reiche, Y. B. Chen, X. Q. Pan, V. Gopala, L. Q. Chen, D. G. Schlom, C. B. Eom, Science **306**, 1005 (2004)
[5] M. E. Lines and A. M. Glass, *Principles and Applications of Ferroelectrics and Related Materials* (Oxford University Press, New York, 1977)
[6] J. Junquera and P. Ghosez, Nature **422**, 506 (2003)
[7] H. X. Fu, R. E. Cohen, Nature, **403**, 281 (2000)
[8] N. A. Pertsev, A. G. Zembilgotov, A. K. Tagantsev, Phys. Rev. Lett. **80**, 1988 (1998)
[9] O. Diéguez, S. Tinte, A. Antons, C. Bungaro, J. B. Neaton, K. M. Rabe, D. Vanderbilt, Phys. Rev. B **69**, 212101 (2004)
[10] W. Zhong, D. Vanderbilt, K. M. Rabe, Phys. Rev. Lett. **73**, 1861 (1994)
[11] W. Zhong, D. Vanderbilt, K. M. Rabe, Phys. Rev. B **52**, 6301 (1995)
[12] U. V. Waghmare, K. M. Rabe, Phys. Rev. B **55**, 6161 (1997)
[13] M. Dawber, P. Chandra, P. B. Littlewood, J. F. Scott, J. Phys.: Condens. Matter, **15**, L393 (2003)
[14] U. V. Waghmare, E. J. Cockayne, B. P. Burton, Ferroelectrics **291**, 187 (2003)
[15] B. P. Burton, E. J. Cockayne, U. V. Waghmare, Phys. Rev B **72**, 064113 (2005)
[16] S. D. Bond, B. J. Leimkuhler, B. B. Laird, J. Comput. Phys. **151**, 114 (1999)

[17] K. Binder, in Phase Transitions and Critical Phenomena, Vol. 5B, edited by C. Domb, M.S. Green, Academic Press (1976)
[18] L. Kim, J. Kim, U. V. Waghmare, D. Jung, J. Lee, Phys. Rev. B **72**, 214121 (2005)
[19] A. M. Bratkovsky and A. P. Levanyuk, Phys. Rev. Lett. **84** 3177; ibid 86 3642 (2001).